

Structure–Property Relationship in Heat-Set Poly(ethylene Terephthalate) Fibers. I. Structure and Morphology

V. B. GUPTA, C. RAMESH, and A. K. GUPTA, *Department of Textile Technology and Centre for Materials Science and Technology, Indian Institute of Technology, Delhi, New Delhi-110016, India*

Synopsis

Poly(ethylene terephthalate) (PET) fibers having a range of structure and morphology were prepared by heat-setting commercial PET yarn at temperatures of 100–250°C for 5 min under two conditions, while the yarn was free to relax and when it was held taut at constant length. The crystallinity, crystallite orientation, and crystallite size were determined by X-ray diffraction while birefringence was measured with the help of optical microscopy. The amorphous orientation factor was computed from the structural parameters. The coupling between the crystalline and amorphous regions was determined using the Takayanagi model. While crystallinity and crystallite orientation values for the corresponding samples of the free-annealed and taut-annealed series did not show very large differences, the free-annealed samples had much lower amorphous orientation, especially when heat-set at higher temperatures. Also while the free-annealed samples showed a predominantly series type of coupling between the crystalline and amorphous regions, the taut-annealed samples showed a significant degree of parallel coupling. It is shown that samples in which there is distinct phase separation between the crystalline and amorphous regions have a predominantly series type coupling.

INTRODUCTION

Heat-setting of poly(ethylene terephthalate) (PET) yarns is an important technological operation; during heat setting the yarn may either be allowed to shrink or held taut at constant length. The comparison of the structures and properties of samples so prepared can lead to an understanding of structure–property relationships in fibers. In an earlier series of papers,^{1–5} data were presented on the structure and elastic, viscoelastic and stress–strain behaviors of PET samples prepared by heat setting of commercial multifilament yarn at temperatures of 100–220°C for times of 1, 15, 30 and 60 min under two conditions, viz., when the yarns were free to relax (designated FA or free-annealed) or when held at constant length (designated TA or taut-annealed). These studies showed that while crystallinity, crystallite orientation, birefringence, and amorphous orientation could account for the observed mechanical properties to some degree, they could not explain the differences in the properties shown by the free- and taut-annealed samples without postulating that the distribution of the crystallites in these two samples was different. No evidence for this difference was then available. However, an analysis of the elastic modulus data showed that while a two-phase series model was satisfactory for the free-annealed samples, it was totally inadequate for the taut-annealed samples. Based on this obser-

vation, it was postulated that while, in the free-annealed samples, the coupling between the crystalline and amorphous regions was likely to be predominantly of the series type, a significant degree of parallel coupling was expected to exist in the taut-annealed samples.

In view of the importance of this morphological factor, viz., the distribution of the crystallites in the semicrystalline fibers, in determining its elastic and viscoelastic³ behavior, and also the transport of dye molecules into the fiber,⁶ investigations into this aspect were considered necessary. With this aim in view a large number of samples was prepared by heat-setting commercial multifilament PET yarn between 100°C and 250°C for 5 min. It may be noted that, in the previously reported work,¹⁻⁵ the maximum temperature of heat setting was 220°C and a heat-setting time of 5 min was not studied. These samples were characterized for crystallinity, crystallite orientation, crystallite size, and birefringence, and from the structural parameters the amorphous orientation factor was computed. Low angle X-ray diffraction studies were also done on these samples. The type of connectivity between the crystalline and amorphous regions was computed in terms of coupling parameters using the Takayanagi model⁷; for this purpose special amorphous samples had to be prepared, and the sonic moduli of these samples were measured. The sonic moduli of the heat-set samples were also measured.

When comparing the data for the free-annealed and taut-annealed samples, two major differences were observed. Among the structural parameters studied, while crystallinity and crystallite orientation for corresponding samples from the two sets had quite close values, the birefringence of the taut-annealed samples was considerably higher than that of the corresponding free-annealed samples, arising mainly from the low orientation of the amorphous phase in these samples. The effect of heat-setting temperature on morphology was also different for the two sets of samples. In the control sample, coupling between the crystalline and amorphous regions was predominantly parallel in nature. This was also the case for the samples of the two sets annealed at the lowest temperature. With increasing temperature of heat setting, while the series component of the coupling increased and the parallel component decreased in both sets of samples, broadly speaking, the free-annealed samples had a predominantly series type of coupling while the taut-annealed samples retained a significant parallel component superimposed over the series component. This was apparently because the free-annealed samples showed greater capacity for phase separation to take place during heat setting, thus making their properties dominated by the amorphous component.

The present paper discusses these structural and morphological aspects; the influence of these factors on the thermal, stress-relaxation, and elastic recovery behaviors of the samples will be the subject of further publications in this series.⁸⁻¹⁰

EXPERIMENTAL

Commercial, drawn multifilament PET yarn 76/36/0, i.e., 76 denier, 36 filaments, and zero twist (draw ratio 3.9) was heat-set in a silicone oil bath maintained at temperatures between 100°C and 255°C under two conditions;

viz., (i) when free to relax (free-annealed, FA) and (ii) when held taut at constant length (taut-annealed, TA) for 5 min.

Crystallinity, crystallite orientation and crystallite size based on (010) plane were determined from X-ray diffraction measurements on the samples, according to the method described earlier.^{1,2}

Birefringence of the samples was measured using an optical microscope and a compensator. The amorphous orientation factor was computed from these parameters using the values of intrinsic birefringence derived elsewhere,¹ viz., $\Delta n_{c0} = 0.29$ and $\Delta n_{a0} = 0.20$, according to the method described earlier.^{1,2}

The sonic moduli, required for determination of the coupling parameters, were measured on a pulse propagation meter at a frequency of 5 kHz. The details of the method are given in an earlier publication.³

Low-angle X-ray diffraction measurements were made on yarn bundles using the low-angle X-ray diffraction facilities at Oak Ridge National Laboratories. It features a rotating-anode X-ray source (Cu K_α radiation), pin-hole collimation of the incident beam, a two-dimensional position sensitive detector, and a minicomputer-based data acquisition and analysis system.

For obtaining the coupling parameters using the model of Takayanagi,⁷ the modulus values of the amorphous samples having different degrees of orientation were required. Amorphous, oriented PET filaments were obtained by cold-drawing a tow in an Instron tensile tester to different draw ratios. Only limited range of draw ratios could be prepared in this way. The sonic moduli of these samples were measured. To obtain data on a wider range, the sonic modulus data of Heuvel and Huisman¹¹ on pre-oriented PET yarn (POY) was combined with these data and the modulus values of oriented, amorphous samples on a wide range of orientation obtained. The amorphous orientation factor f_{am} was determined through the use of eq. (5) (stated subsequently) using the crystallinity $\beta = 0$ and intrinsic birefringence of amorphous phase, $\Delta n_{am} = 0.20$.

THEORY

The general model of Takayanagi⁷ is illustrated in Figures 1(a) and (b), which are equivalent. The fiber modulus is given by

$$E_f = \lambda \left[\frac{\phi}{E_c} + \frac{1-\theta}{E_a} \right]^{-1} + (1 - \lambda)E_a \quad (1)$$

where λ and ϕ are measures of series and parallel coupling, respectively, and E_c and E_a are the effective crystalline and amorphous moduli, respectively. The degree of crystallinity, β , equals $\lambda\phi$. For the two extreme cases, the expressions take the following forms:

Series coupling, $\lambda = 1$:

$$\frac{1}{E_f} = \frac{\beta}{E_c} + \frac{(1 - \beta)}{E_a} \quad (2)$$

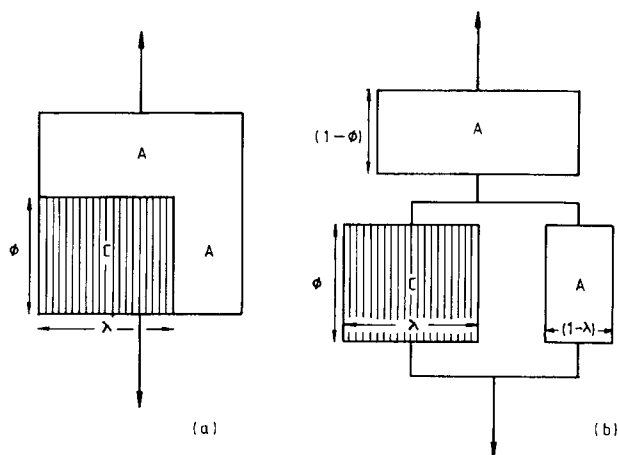


Fig. 1. Two mutually equivalent schematic representations of a partially crystalline polymer system by a unit cube mechanical model system by Takayanagi.⁷ A = amorphous; C = crystalline.

Parallel coupling, $\phi = 1$:

$$E_f = \beta E_c + (1 - \beta) E_a \quad (3)$$

The effective crystalline modulus E_c was calculated using the following expression¹²:

$$\frac{1}{E_c} = \frac{\sin^4 \theta}{E_c^t} + \frac{\cos^4 \theta}{E_c^l} + \sin^2 \theta \cos^2 \theta \left[\frac{1}{G_c^t} - \frac{2\nu_{tt}}{E_c^l} \right] \quad (4)$$

where θ represents an average of the angle which the c -axis of the crystallite makes with the fiber axis. The average value of θ was determined from X-ray diffraction studies of each sample from the Hermans' orientation factor f_c , which can be written as

$$f_c = 1 - \frac{3}{2} \sin^2 \theta$$

The values of the other constants for the crystal for each sample were assumed to be^{12,13} transverse modulus $E_c^t =$ shear modulus $G_c^t = 3.68 \times 10^{10}$ dyn/cm², longitudinal modulus $E_c^l = 13.7 \times 10^{11}$ dyn/cm², Poisson's ratio $\nu_{tt} = 0.50$. The effective amorphous modulus E_a , was determined from the experimentally obtained moduli of the cold-drawn amorphous tow or POY yarn having a corresponding orientation factor.

Using the sonic modulus values of the fiber, E_f , the value of λ and ϕ , the series and parallel coupling parameters can now be determined for all the samples using eq. (1).

RESULTS AND DISCUSSION

The crystallinity, crystallite size, and crystallite orientation data are presented in Figure 2. It may be noted that in both sets of samples (FA and TA), while crystallinity and crystallite size increase by a factor of 2 or more

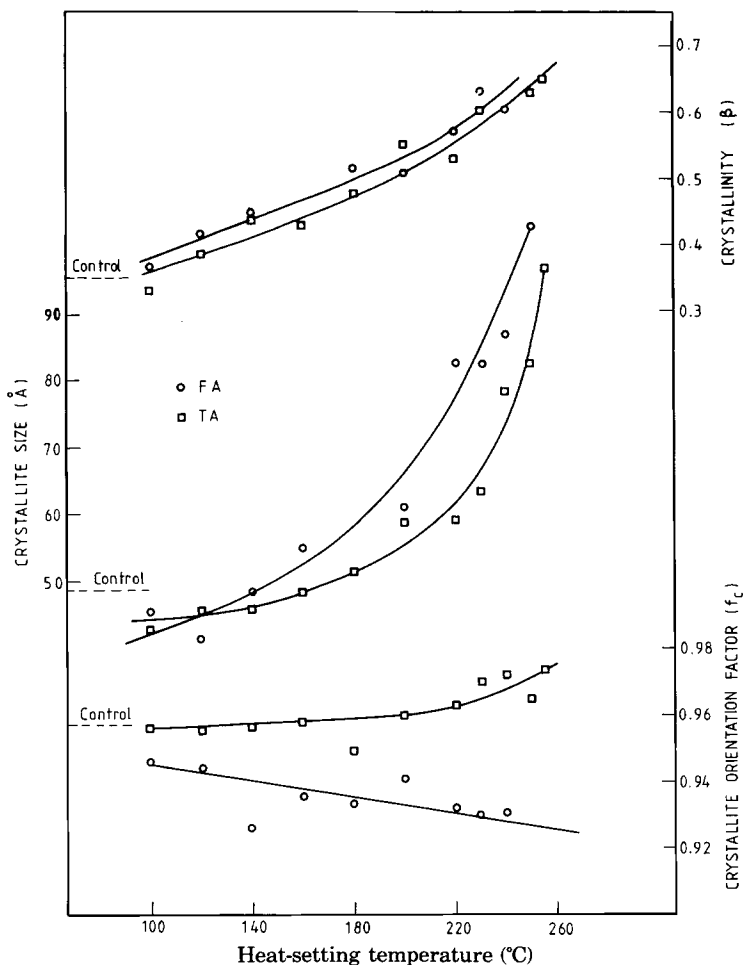


Fig. 2. X-ray crystallinity, crystallite size corresponding to (010) plane, and Hermans' crystallite orientation factor (f_c) as a function of heat setting temperature.

over the studied range of heat-setting temperatures, crystallite orientation shows only a very slight change. Thus the increase in crystallinity, accompanied by an increase of crystallite size, does not involve any significant disorientation of the crystallites in the free-annealed samples; in the taut-annealed samples crystallite orientation may not change or may in fact improve slightly.

The birefringence data (Fig. 3) show that orientation improves with increasing heat-setting temperature for taut-annealed samples, and decreases for free-annealed samples. It may, however, be noted that the lowest value of birefringence for free-annealed samples is 0.163, which is indicative of considerable molecular orientation being retained in the sample even at the higher temperatures of heat setting. The amorphous orientation factors for the various samples are shown in Figure 3. It may be noted that, in the taut-annealed samples, amorphous orientation decreases slightly with increasing heat setting temperature in spite of the increase in birefringence. Also in the free-annealed samples, amorphous orientation shows consid-

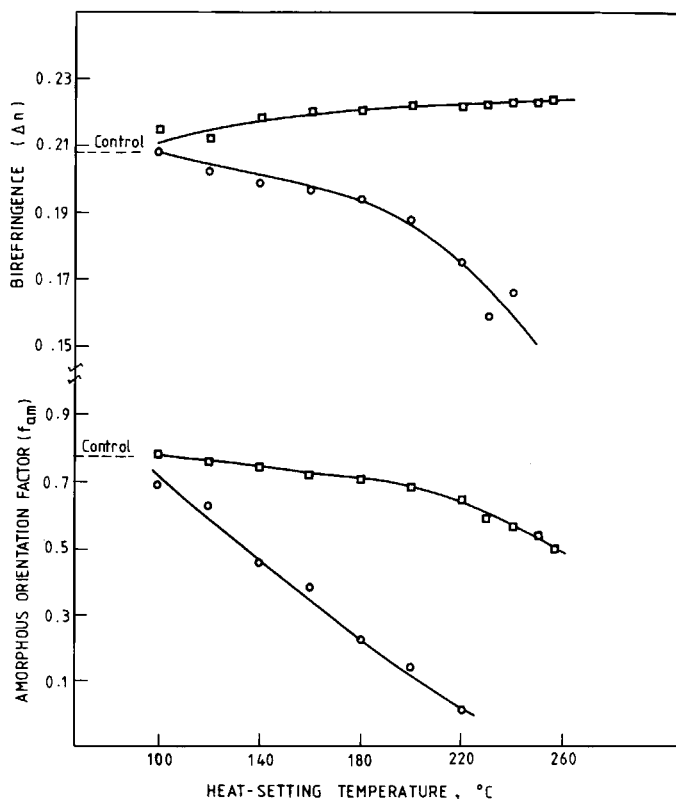


Fig. 3. Birefringence (Δn), and Hermans' amorphous orientation factor (f'_{am}) as a function of heat setting temperature. (○) FA; (□) TA.

erable decrease, and the free-annealed samples heat-set at high temperatures have very low amorphous orientation values. In fact, the parameter most affected by heat setting is the amorphous orientation factor of the free-annealed samples.

The low angle X-ray diffraction data are presented in Figures 4 and 5. The equiintensity contour maps, shown in Figure 4 for some cases, of the LAXS data reveal the occurrence of two-point pattern only at higher temperatures of heat setting in both FA and TA samples. The control and the samples heat-set at temperatures up to 180°C show only central scattering pattern. It is noteworthy that compared to the TA samples, the appearance of the two-point pattern is at a relatively lower heat setting temperature in the case of the FA samples. Intensity of the two-point pattern increased with increasing heat setting temperature. The intensity profile of the two-point pattern along the meridian for the various samples are shown in Figures 5(a) and (b). The appearance of the two-point pattern is an indication of the formation of distinct separation of crystalline and amorphous phases. Thus the crystalline and amorphous regions are not distinctly separated with clear phase boundaries in the control sample or in samples heat-set at lowest temperatures. Heat setting at higher temperatures results in phase separation and is more marked for free-annealed samples. The long period of some of the fibers could be calculated from the intensity profiles

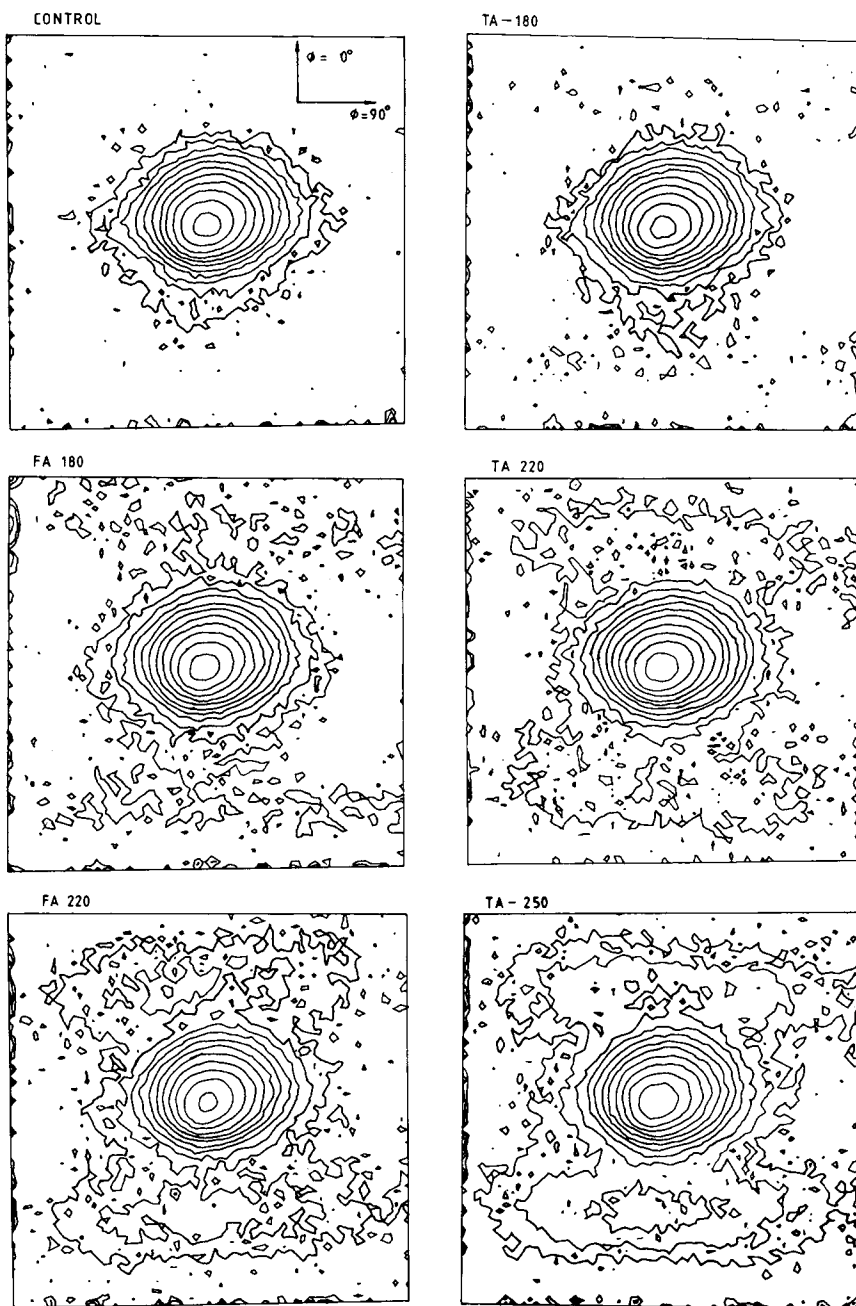


Fig. 4. LAXS equi-intensity contour maps for control and some heat-set samples of PET fibers.

[Figs. 5(a) and (b)] and are shown in Table I. The long periods and half-widths obtained on our samples are quite close to the values quoted by Fakirov et al.¹⁴ for similar samples of PET.

The sonic moduli of the amorphous samples, prepared by cold drawing of a PET tow to various draw ratios and of preoriented PET yarn¹¹ with

different degrees of orientation, are shown in Figure 6. These values of amorphous modulus were used in the calculation of coupling parameters λ (series) and ϕ (parallel) for the various samples using eq. (1). The coupling parameters are shown in Table II; for the sake of completeness, the other parameters which form part of these calculations, are also included in Table II. These parameters are f_{am} , the Hermans' amorphous orientation factor, f_c , the Herman's crystalline orientation factor, θ , the average angle between the crystallite axis and the fiber axis as calculated from f_c , β , the degree of crystallinity, E_c , the effective crystalline modulus, E_a , the effective amorphous modulus, and E_f , the measured sonic modulus.

The coupling parameters, λ (series) and ϕ (parallel), are plotted for the FA and TA samples in Figure 7, the values for the control sample are also indicated in the figures.

It is seen that the control sample shows a very high degree of parallel coupling. It may be recalled that the low-angle X-ray diffraction of this sample is very weak and diffuse, indicating absence of distinct phase separation between the crystalline and amorphous regions in this sample. The sample heat-set at the lowest temperature also shows features similar to

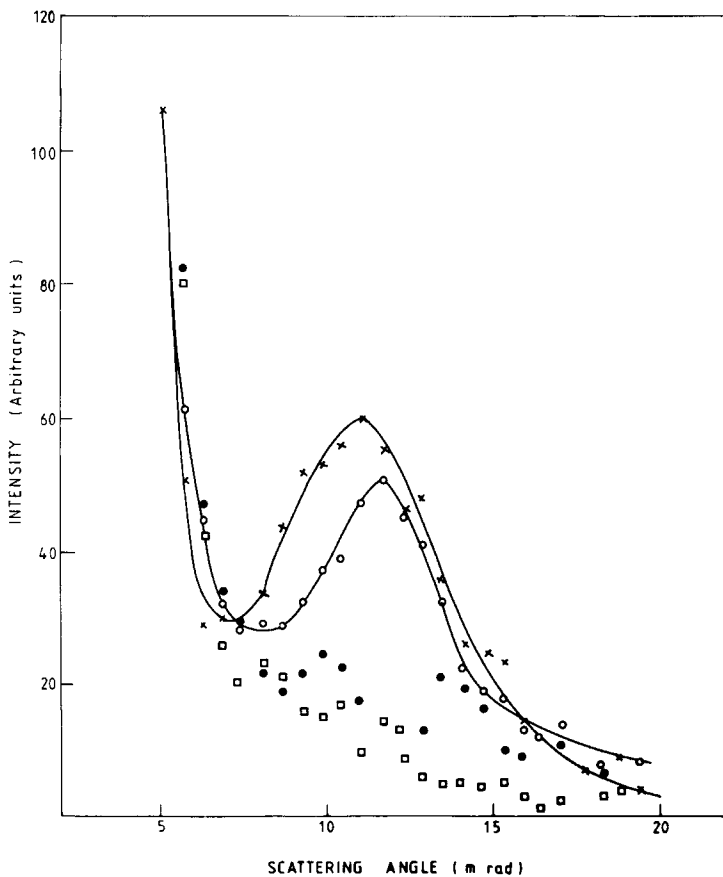


Fig. 5(a). LAXS intensity profile for free-annealed PET fiber samples: (\square) control; (\bullet) FA-180; (\times) FA-200; (\circ) FA-220.

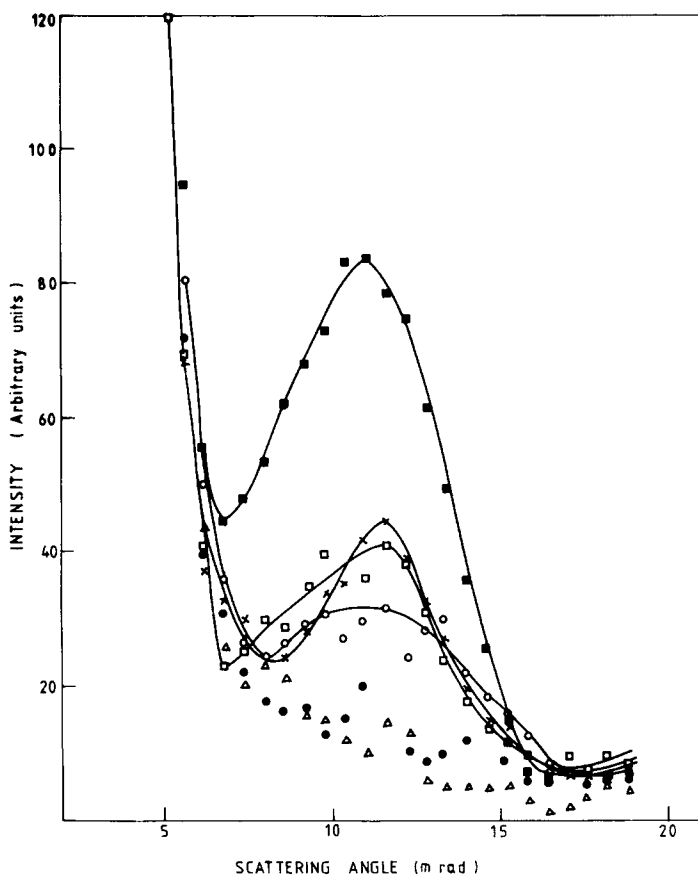


Fig. 5(b). LAXS intensity profile for taut-annealed PET fiber samples: (Δ) control; (\bullet) TA-180; (\circ) TA-220; (\times) TA-230; (\square) TA-240; (\blacksquare) TA-250.

the control sample both from the Takayanagi model calculation of λ and ϕ and from the low-angle X-ray diffraction studies. With increase in the heat setting temperature, as the semicrystalline structure of the fiber reorganizes, λ , the series coupling parameter, increases while ϕ , the parallel coupling parameter, decreases in both sets of samples (FA and TA). It is instructive to see how the ratio of parallel to series coupling parameters, ϕ/λ , varies with heat setting temperature; as shown in Figure 8, this ratio decreases with increasing heat setting temperature, but the values for taut-annealed samples are always higher than the values for corresponding free-

TABLE I
Values of Long Period and Half-Width from LAXS Data

Sample	Long period (\AA)	Half-width $\times 10^{-3}$ (rad)
TA 230	133	3.4
TA 240	133	4.7
TA 250	140	5.2
FA 220	131	3.5
FA-230	140	4.6

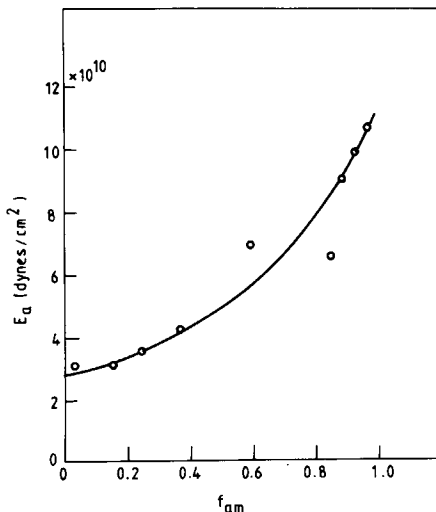


Fig. 6. Sonic moduli of oriented amorphous fibers as a function of Hermans' amorphous orientation factor (f_{am}).

annealed samples all through the temperature range studied. Thus, broadly speaking, while the free-annealed samples may be characterized by a predominantly series type of coupling, the taut-annealed samples have a substantial parallel component superimposed on the series coupling. Recent work reported by Fontaine et al.¹⁵ on isothermally crystallized isotropic PET and by Fakirov et al.¹⁴ on isothermally annealed highly oriented PET assists in the interpretation of the coupling parameters in terms of sample morphology. These authors have shown that isothermal annealing around 200°C and above results in a crystal thickening process without change in long period, and this was attributed to crystal perfection phenomenon at the boundary layers of the crystalline and amorphous phases close to the folds. This reorganization has been shown to result in sharpening up of the folded structure and smoothening of the amorphous interface.¹⁵ The structural features result in more distinct phase separation, and it is obvious that they will enhance the series coupling parameter. In the present investigations, phase separation occurs in both sets of samples and is accompanied by disorientation of the amorphous regions; the effects are marked for the free-annealed samples. The measured sonic moduli for the two sets of samples are plotted in Figure 9 along with those predicted by the Takayanagi model for the ideal cases of complete series ($\lambda = 1$) and complete parallel ($\phi = 1$) coupling. It is seen that while the moduli of the free-annealed samples are close to those predicted by series coupling, in the taut-annealed samples this is the case only for samples heat-set at the highest temperatures of heat setting used in this study. This indicates that heat setting under constraints allows phase separation to occur only at the higher temperatures; a conclusion which was arrived at by Statton et al.¹⁶ from the low-angle X-ray diffraction studies. The sonic moduli of all the samples are shown in Figure 10 as a function of the ratio ϕ/λ and it is seen that the higher this ratio the higher the modulus, as would be expected.

TABLE II
Structural Parameters and Coupling Parameters for Various Heat-Set and Control PET Fiber Samples

Sample	Structural parameters					Sonic modulus $\times 10^{11}$ (dyn/cm ²)					Coupling parameters		
	β	f_c	θ	f_{am}	E_c	E_o	E_f	λ	φ	φ/λ			
Control	0.36	0.96	9.8	0.78	6.91	0.75	1.76	0.41	0.86	2.08			
TA	0.33	0.96	9.9	0.77	6.84	0.74	1.73	0.38	0.87	2.29			
120	0.39	0.96	10.0	0.76	6.76	0.71	1.66	0.48	0.83	1.73			
140	0.44	0.96	9.9	0.74	6.84	0.69	1.78	0.53	0.83	1.58			
160	0.43	0.96	9.6	0.72	6.99	0.68	1.61	0.54	0.80	1.48			
180	0.48	0.95	10.6	0.70	6.33	0.65	1.62	0.61	0.79	1.31			
200	0.55	0.96	9.4	0.68	7.16	0.64	1.64	0.73	0.75	1.03			
220	0.53	0.96	9.0	0.64	7.43	0.60	1.55	0.70	0.75	1.07			
230	0.60	0.97	8.1	0.58	8.14	0.56	1.55	0.81	0.74	0.91			
240	0.61	0.97	7.9	0.56	8.36	0.54	1.53	0.83	0.74	0.89			
250	0.63	0.97	8.8	0.54	7.62	0.53	1.52	0.85	0.74	0.87			
255	0.65	0.97	7.7	0.49	8.48	0.49	1.51	0.82	0.76	0.93			
FA	0.37	0.95	11.0	0.69	6.07	0.64	1.32	0.48	0.77	1.61			
120	0.42	0.94	11.1	0.62	6.01	0.58	1.18	0.60	0.70	1.18			
140	0.45	0.93	12.8	0.46	5.09	0.47	0.86	0.78	0.58	0.74			
160	0.48	0.94	12.0	0.38	5.51	0.43	0.81	0.87	0.55	0.64			
180	0.51	0.93	12.1	0.22	5.46	0.34	0.68	0.91	0.56	0.62			
200	0.51	0.94	11.4	0.14	5.84	0.31	0.63	0.92	0.55	0.60			
220	0.57	0.93	12.3	0.00	5.36	0.28	0.56	1.18	0.49	0.41			

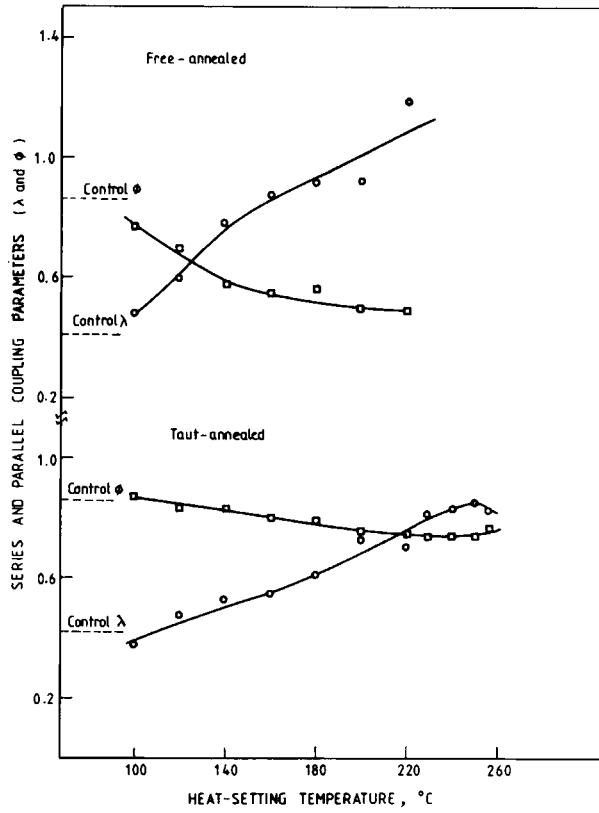


Fig. 7. Coupling parameters, λ (series) (○) and ϕ (parallel) (□), as function of heat-setting temperature.

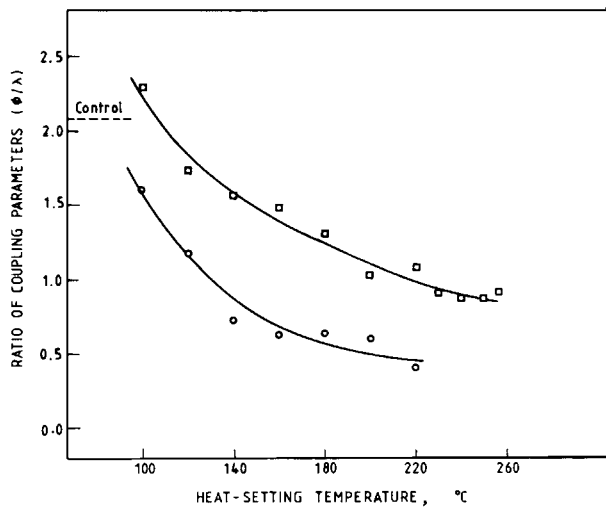


Fig. 8. Ratio of parallel to series coupling (ϕ/λ) as a function of heat-setting temperature: (○) FA; (□) TA.

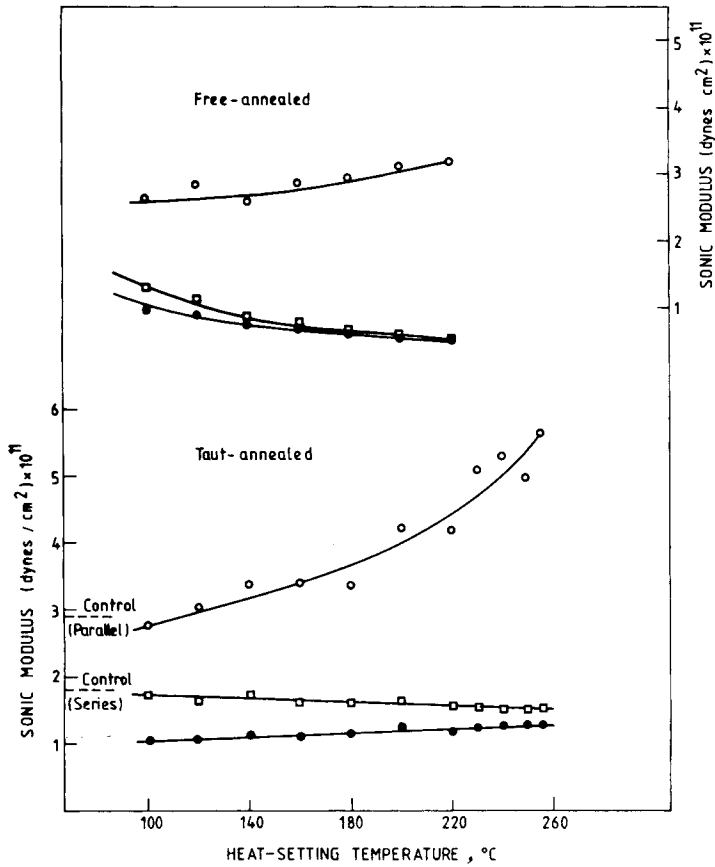


Fig. 9. Comparison of experimental and predicted sonic modulus data for FA and TA samples: (●) series; (○) parallel; (□) experimental.

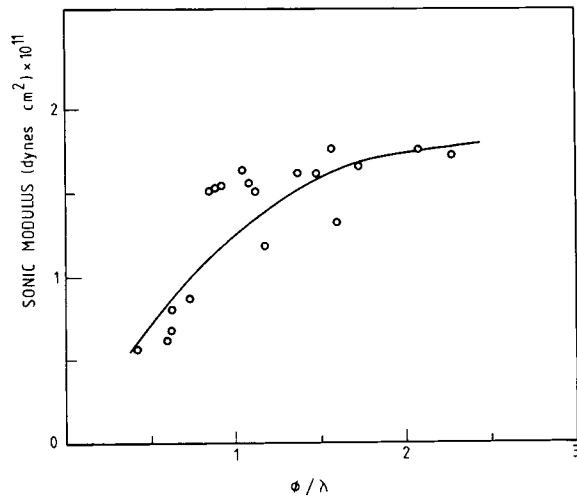


Fig. 10. Variation of sonic moduli as a function of ϕ/λ obtained from the data on all the samples.

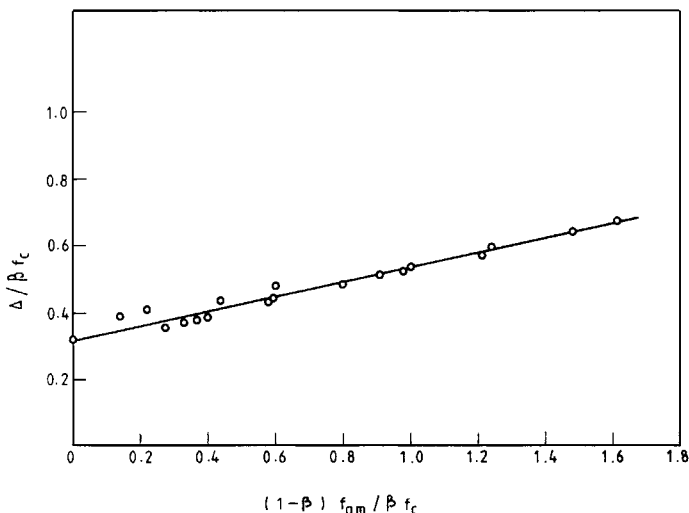


Fig. 11. Plot from the present data for calculation of intrinsic birefringence for the crystalline and amorphous phases. The line represents the best fit by least squares fit method.

In the present calculations of structural and morphological parameters, the values of intrinsic birefringence that have been used are: $\Delta n_{c_0} = 0.29$ and $\Delta n_{am_0} = 0.20$, taken from an earlier publication¹ based on data for 30 samples heat-set from 100°C to 220°C. These values of intrinsic birefringence were calculated from the measured birefringence, Δn , using the following equation¹:

$$\Delta n = \beta \Delta n_{c_0} f_c + (1 - \beta) \Delta n_{am_0} f_{am} \quad (5)$$

where β is the degree of crystallinity, f_c is the Hermans' crystallite orientation factor, and f_{am} the Herman's amorphous orientation factor. Equation (5) may be rewritten as

$$(\Delta n / \beta f_c) = \Delta n_{c_0} + \Delta n_{am_0} (1 - \beta) (f_{am} / \beta f_c) \quad (6)$$

If $\Delta n / \beta f_c$ is plotted against $(1 - \beta) f_{am} / \beta f_c$, the slope and intercept directly give the values of Δn_{am_0} and Δn_{c_0} , respectively. Such a plot for the present samples (17 in number) is shown in Figure 11, and the data fall on a straight line with $\Delta n_{c_0} = 0.31$ and $\Delta n_{am_0} = 0.21$. These are very close to the intrinsic birefringence values used in the analysis of the present data, viz., $\Delta n_{c_0} = 0.29$, $\Delta n_{am_0} = 0.20$. The small difference in the values of intrinsic birefringence did not result in any significant difference in the data presented.

It will be shown in series of publications to follow⁸⁻¹⁰ that the thermal, stress-relaxation, and recovery behaviors of heat-set PET yarns are determined to a very large extent by the structural and morphological factors described in this publication. However, the data are not yet sufficient to propose satisfactory models for TA and FA samples. At the moment, it can only be stated that, in addition to structural parameters like crystallinity, crystallite orientation, birefringence, and amorphous orientation, morphological factors like the distribution of crystallites in the sample must

also be taken into account when models are designed to predict fiber properties. It is hoped that further work in progress on such samples will assist in developing an appropriate model.

The authors are grateful to Dr. N. B. Patil and Dr. P. K. Chidambareswaran for their assistance in carrying out the X-ray diffraction studies at Cotton Technological Research Laboratories, Bombay. They are also grateful to Dr. Ping Young and Dr. Satish Kumar of UMass, Amherst, for the LAXS measurements.

References

1. V. B. Gupta and S. Kumar, *J. Polym. Sci., Part A-2*, **17**, 1307 (1979).
2. V. B. Gupta and S. Kumar, *J. Appl. Polym. Sci.*, **26**, 1865 (1981).
3. V. B. Gupta and S. Kumar, *J. Appl. Polym. Sci.*, **26**, 1877 (1981).
4. V. B. Gupta and S. Kumar, *J. Appl. Polym. Sci.*, **26**, 1885 (1981).
5. V. B. Gupta and S. Kumar, *J. Appl. Polym. Sci.*, **26**, 1897 (1981).
6. V. B. Gupta, M. Kumar, and M. L. Gulrajani, *Text. Res. J.*, **45**, 463 (1975).
7. M. Takayanagi, *Proceedings of the 4th International Congress on Rheology, Part I*, Wiley-Interscience, New York, 1965, p. 161.
8. V. B. Gupta, C. Ramesh, and A. K. Gupta, *J. Appl. Polym. Sci.*, to appear.
9. V. B. Gupta, C. Ramesh, and A. K. Gupta, *J. Appl. Polym. Sci.*, to appear.
10. V. B. Gupta, C. Ramesh, and A. K. Gupta, *J. Appl. Polym. Sci.*, to appear.
11. H. M. Heuvel and J. Huisman, *J. Appl. Polym. Sci.*, **22**, 2229 (1978).
12. I. M. Ward, *Mechanical Properties of Solid Polymers*, Wiley-Interscience, London, 1971.
13. D. C. Prevorsek, R. H. Butler, Y. D. Kwon, G. E. R. Lamb, and R. K. Sharma, *Text. Res. J.*, **47**, 107 (1977).
14. S. Fakirov, E. W. Fischer, R. Hoffman, and G. F. Schmidt, *Polymer*, **18**, 1121 (1977).
15. F. Fontaine, J. Ledent, G. Groeninckx, and H. Reynaers, *Polymer*, **23**, 185 (1982).
16. W. O. Statton, J. L. Koenig, and M. Hannon, *J. Appl. Phys.*, **41**, 4290 (1970).
17. R. J. Samuels, *Structured Polymer Properties*, Wiley, New York, 1974.

Received October 20, 1983

Accepted February 4, 1984